

FORMATION AND TIDAL EVOLUTION OF HOT SUPER-EARTHS IN MULTIPLE PLANETARY SYSTEMS

Ji-Lin Zhou¹

Abstract. Hot super-Earths are exoplanets with masses $\leq 10M_{\oplus}$ and orbital periods ≤ 20 days. Around 8 hot super-Earths have been discovered in the neighborhood of solar system. In this lecture, we review the mechanisms for the formation of hot super-Earths, dynamical effects that play important roles in sculpting the architecture of the multiple planetary systems. Two example systems (HD 40307 and GJ 436) are presented to show the formation and evolution of hot super-Earths or Neptunes.

1 Introduction

More than 330 exoplanets have been detected in the neighborhood of solar system by various techniques, especially by radial velocity measurements¹. Among them, hot super-Earths(HSEs hereafter) are characterized with masses $\leq 10M_{\oplus}$ (Earth mass) and orbit periods ≤ 20 days. The mass upper limit is set based on the critical mass ($\sim 10M_{\oplus}$) in the core-accretion scenario of giant planet formation, above which efficient gas accretion will set in(Pollack et al. 1996). The period upper limit (20 days, or ~ 0.15 AU) is set with somewhat arbitrary, where the temperature of a solid body due to the radiation of a solar-mass star is ~ 730 K, and the tidal circularization timescale of a $10M_{\oplus}$ solid planet is ~ 13 Gyrs, thus tidal dissipation is effective for solid planets inside this orbit.

To date, only 8 HSEs are detected, with 13 hot Neptunes (HNs hereafter) which have similar orbital periods (< 20 days) but larger masses. These 21 HSEs and HNs are distributed in 15 planetary systems, among them there are 5 single-planet systems up to the present observations: GJ 436, GJ 674, HD 219828, HAT-P-11, HD 285968, HD4308; the others are in multiple planet systems(Fig.1.). Due to the limit number of HSEs and HNs, a statistical study of the orbital parameters for HSEs is still unreliable.

¹ Department of Astronomy, Nanjing University, Nanjing 210093, China,zhoujl@nju.edu.cn
¹<http://exoplanet.eu/>

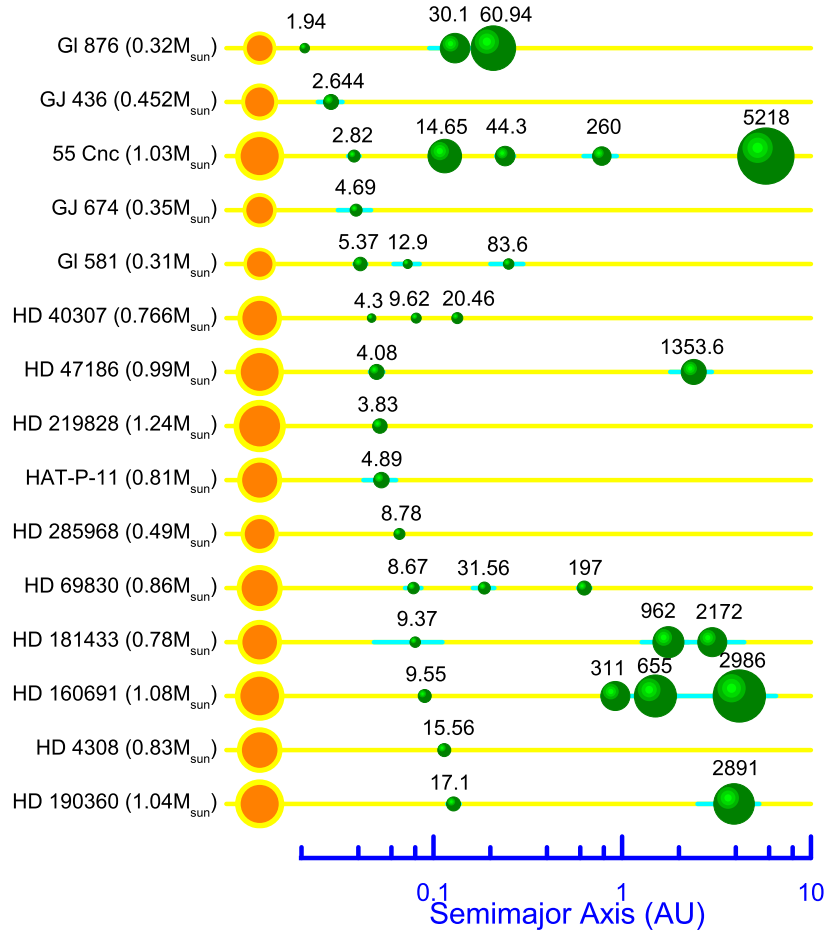


Fig. 1. Diagram of semimajor axes and masses for the 15 known hot super-Earth and Neptune systems. The diameters depicted for planets and stars are proportional to the cube root of the planetary $M \sin i$ and stellar mass, respectively. The periape to apoapse excursion is shown by a horizontal line intersecting the planet. Labels around the planets are their orbital periods in units of days. Data are from <http://exoplanet.eu/>.

One interesting problem is the formation of HSEs. According to the core-accretion model of planet formation (Safronov 1969, Pollack et al. 1996), planetesimals coagulate via runaway growth and become protoplanetary embryos through

runaway and oligarchic growth (Kokubo & Ida 1996, Kokubo & Ida 2002). When one adopts the empirical minimum mass solar nebula model (hereafter MMSN), the surface density of gas and the heavy elements are expressed as (Hayashi 1981, Ida & Lin 2004),

$$\Sigma_g = 2.4 \times 10^3 f_g \left(\frac{a}{1\text{AU}}\right)^{-3/2} \text{ g cm}^{-2}, \quad (1.1)$$

and

$$\Sigma_d = 10 f_d \gamma_{\text{ice}} \left(\frac{a}{1\text{AU}}\right)^{-3/2} \text{ g cm}^{-2}, \quad (1.2)$$

respectively, where a is the semi-major axis, f_g and f_d are enhancement factors, γ_{ice} is the volatile enhancement with a value of 4.2 or 1 for exterior or interior to the snow line (where temperature is 170K due to the stellar radiation), respectively. In such a disk, the growth timescale of a planetary embryo with mass M is estimated as (Kokubo & Ida 2002),

$$\tau_{\text{growth}} \simeq 0.12 \gamma_{\text{ice}}^{-1} f_d^{-1} f_g^{-2/5} \left(\frac{a}{1\text{AU}}\right)^{27/10} \left(\frac{M}{M_{\oplus}}\right)^{1/3} \left(\frac{M_*}{M_{\odot}}\right)^{-1/6} \text{ Myr}, \quad (1.3)$$

where M_* is the stellar mass. In the ideal situation that planetesimals do not undergo significant orbital decay, the growth of embryos are stalled with isolation masses (Ida & Lin 2004),

$$M_{\text{iso}} = 0.16 f_d^{3/2} \gamma_{\text{ice}}^{3/2} \left(\frac{\Delta_{\text{fz}}}{10R_h}\right)^{3/2} \left(\frac{a}{\text{AU}}\right)^{3/4} \left(\frac{M_*}{M_{\odot}}\right)^{-1/2} M_{\oplus}, \quad (1.4)$$

when they cleaned the planetesimals within their feeding-zone of width $\Delta_{\text{fz}} \sim 10 - 12R_h$, where $R_h = (2M/3M_*)^{1/3}a$ are their mutual Hill's radii. The orbital crossing timescale for a swarm of isolated embryos with equal mass ratios $\mu = M_{\text{iso}}/M_*$ is fitted by numerical simulations (Zhou et al. 2007)

$$\log\left(\frac{T_c}{P_m}\right) = A + B \log\left(\frac{\Delta_{\text{fz}}}{2.3R_h}\right), \quad (1.5)$$

where

$$A = -2 - 0.27 \log \mu, B = 18.7 + 1.1 \log \mu, \quad (1.6)$$

and P_m is the period of the middle planet (~ 10 days for HSE). For a moderate disk with $f_d = 2$ and feeding zone width of $12R_h$, the mass of an isolated embryo at 10 day's orbit is $M_{\text{iso}} = 0.08M_{\oplus}$ with a very short growth time (within 100 years), however, the orbital crossing timescale for such a swarm of embryos is ~ 7 Gyr by Eq.(1.5), which it is quite stable unless extra perturbations excite their eccentricities. Considering the observed HSEs, the interesting question is: how do they form from a swarm of isolated embryos?

2 Formation Scenarios of HSE

Several scenarios for the formation of HSEs are summarized in Raymond et al. (2008). There are three major sources of HSEs: (i) embryos shepherded into the

mean motion resonances by inward migration of gas giants in outside orbits(Zhou et al. 2005, Fogg & Nelson 2005), (ii) embryos shepherded by the secular resonances between gas giants during the depletion of gas disk(Zhou et al. 2005, Nagasawa et al. 2005). In these two mechanisms, the eccentricities of the embryos are excited in resonances, which results in their merge and growth to HSEs. (iii) inward type I migration of super-Earth protoplanets to hot orbits. As we can see from eq.(1.4), in situ formation of HSEs requires a large solid mass ($f_d \geq 10$), which is unlikely unless type I migration of embryos are effective. In fact, for a specific system, all these effects (type I migration, gas giant perturbation or disk depletion, tidal dissipation, etc.) may account for making the architecture of a planet system with HSEs. We discuss several major effects in the following text.

2.1 Type I migration

One of the major obstacle for the core-accretion scenario is the fast migration of Earth mass embryos. For such a planet embedded in a geometrically thin protoplanetary disk, angular momentum exchanges between the planet and nearby gas disk will cause a net momentum lose on the planet, which results in a so called type I migration of the planet with a timescale(Goldreich & Tremaine 1979, Ward 1997, Tanaka et al. 2002),

$$\tau_{\text{I-mig}} \simeq \frac{1}{C_1(1.1\beta - 2.7)} \left(\frac{M_*}{M}\right) \left(\frac{M_*}{\Sigma_g a^2}\right) \left(\frac{H}{a}\right)^2 \left(\frac{P_K}{2\pi}\right) \quad (2.1)$$

where negative/positive values of $\tau_{\text{I-mig}}$ corresponds inward/outward migration respectively, M , P_K and H are the embryo's mass, Keplerian period and thickness of the protostellar disk, respectively, $\beta \equiv \partial \ln \Sigma_g / \partial \ln a$ and $C_1 (\sim 0.03 - 0.1)$ is a reduction factor. According to Eq. (2.1), the migration timescale is 0.05 Million years for a Earth mass planet at 1AU. Such a fast migration will evacuate the embryos so that no gas giant will form through core-accretion scenario, unless the migration speed is at least an order of magnitude smaller(Alibert et al. 2005, Ida & Lin 2008). How to reduce the speed of type I migration is a key issue of present planet formation theory.

Recent hydrodynamical simulation indicates that type I inward migration can be stopped near a boundary of a density maximum(Masset et al. 2006). During the orbital decay of a protoplanet, the exchange of angular momentum between it and the fluid elements that perform U-turn at the end of the horseshoe streamlines generates a corotation torque on the protoplanet(Ward 1991, Masset 2002). The quantity of corotation torque, $\Gamma_c \propto \Sigma_g d \ln(\Sigma_g/B) / d \ln a$, depends on the local gradient of the disk surface, where B is the Oort constant and $B \sim a^{-3/2}$ in a near Keplerian motion. At the surface density increment, the corotation torque of the disk is positive. Simulations indicate that a disk-surface-density jump of about 50% over 3-5 disk thicknesses suffices to cancel out the negative Lindblad torque that generates the type I migration, leading the density maximum a "trap" of protoplanet(Masset et al. 2006).

Several locations of the protoplanetary disk can serve as the density maximums, e.g., the *inner disk cavity* due to the stellar magnetic field. Around the corotation radius, the stellar magnetic torque acts to extract angular momentum from the disk and spins down the disk material. At the location where the stellar magnetic field completely dominates over disk internal stresses, sub-Keplerian rotation leads to a free-fall of disk material on to the surface of the star in a funnel flow along magnetic-field lines, results in an inner disk truncation (Königl 1991). The maximum distance of disk truncation is estimated at 9.1 stellar radii. Considering the radius of protostar is generally 2-3 times larger than their counterpart in main sequence, the inner disk truncation would occur at $\sim 0.1\text{AU}$. Once the embryo has spiral in the inner disk cavity, type I migration is greatly reduced according to equation (2.1), thus migration is effectively stopped.

Another place is the *Boundary of MRI active-dead zones*. During the classical T Tauri stars (CTTS) phase, magnetorotational instability (MRI) is effective so that the gas disk has a layered structure as a sandwich: inside the boundary, the protostellar disk is thermally ionized while outside this boundary, only the surface layer (with a thickness $\cong 100\text{g cm}^{-2}$) is ionized by stellar X-rays and diffuse cosmic rays, leaving the central part of the disk a highly neutral and inactive “deadzone” (Balbus & Hawley 1991, Gammie 1996). Near the boundary of active and dead zone, a positive density gradient is expected (Kretke & Lin 2007, Kretke et al. 2009). In fact, adopt the ad hoc α -prescription for the protoplanetary gas disk (Shakura & Sunyaev 1973), the effective viscosity of the disk is written as $\nu = \alpha c_s h$, where c_s and $h = c_s/\Omega_K$ are the sound speed of midplane and the isothermal density scale height, respectively. The magnitude of α increases about two times from magnetic saturated regions (~ 0.006) to active ones (~ 0.018). Assuming a constant mass accretion rate ($\dot{M}_g = 3\pi\nu\Sigma_g$) across the disk, the variation of viscosity ν indicates Σ_g could increase two times from MRI dead zone to active zone. The sharp increase of column density across the boundary helps to halt the embryos under type I migration.

According to the above discussions, the inward migration of type I can be halted at some specific location of the disk before gas depletion. The observation of HSEs, e.g., HD 40307 system (section 3.1), gives a clear evidence for the migration-and-halt history.

2.2 Perturbations from planet companions

As we have shown in Eq.(1.4), embryos outside the snow line tend to have large isolation masses. When their masses exceed the critical mass ($\sim 10M_\oplus$) so that efficient gas accretion will set in, they will grow to gas giants in a timescale of million years, leaving a group of isolated embryos with masses $\sim 0.1M_\oplus$ inside the snow line. During and after the formation of gas giants, their evolution will greatly affect the subsequent formation of super-Earths. There are two major types of perturbations to these embryos:

Shepherding in Mean Motion Resonance (MMR). During the type II migration of gas giants, the locations of inner mean motion resonances (mainly 2:1 MMR)

with the gas giants will sweep through inner disk, trap and shepherd the embryos, excite their eccentricity, which results in the merge of isolated embryos and formation of HSEs(e.g., Zhou et al. 2005). The resonance trap and shepherding is efficient as long as the timescale of type II migration(Ida & Lin 2004),

$$\tau_{\text{II}} = 0.8\text{Myr} f_g^{-1} \left(\frac{M_p}{M_J}\right) \left(\frac{M_\odot}{M_*}\right) \left(\frac{\alpha}{10^{-4}}\right)^{-1} \left(\frac{a_p}{1\text{AU}}\right)^{1/2}, \quad (2.2)$$

is much longer than the libration period (typically less than hundreds of years inside the snow line), where M_p, a_p are the mass and semi-major axis of the gas giant. Prior to severe gas depletion, the eccentricities of the embryos are damped on a timescale(Ward 1993),

$$\tau_{e,\text{damp}} \simeq 300 f_g^{-1} \left(\frac{M}{M_\oplus}\right)^{-1} \left(\frac{a}{1\text{AU}}\right)^2 \text{yr}. \quad (2.3)$$

The eccentricity damp of embryos enhances the trap of 2:1 MMR, as the resonance region for circular orbits is relatively wider. However, when type I migration of embryos are taken into consideration, whether they will stop at 2:1 MMR or other MMRs with higher orders depends on the migration speed of embryos, as we will see in section 3.1 for HD 40307 system.

After the embryos become super-Earths, their orbits may perturb each other, or they can accrete gas to become giant planets, if there exists efficient gas in the disk. The embryos themselves may trap into resonance through type I migration. Recently simulations indicate that resonance trap between embryos are common during the migration of embryos (Terquem & Papaloizou 2007, Fogg & Nelson 2007, Morbidelli et al. 2008, Lin et al. 2009).

Secular perturbations between two planets (or embryos) in non-resonance orbits exchange their angular momentums, modulate their eccentricities, leaving their semi-major axes almost unchanged. Under the perturbation of an outer planet (M_2) with semi-major axes a_2 and eccentricity e_2 , the maximum eccentricity (e_1) of the inner planet (M_1) that can achieve from an initial circular orbit a_1 is,

$$e_{1\text{max}} = \frac{5}{2} e_2 \varepsilon_2^{-2} \left(\frac{a_1}{a_2}\right) \left| 1 - \varepsilon_2^{-1} \sqrt{\frac{a_1}{a_2}} \left(\frac{M_1}{M_2}\right) + \gamma \varepsilon_2^3 \right|^{-1}. \quad (2.4)$$

where $\varepsilon_2 = \sqrt{1 - e_2^2}$, γ is the ratio of general relativity to companion perturbation on periapsis precession of M_1 (Mardling 2007). This equation can be used to locate an approximate region of the planet companion in either nearby or distance orbits, while general three-body simulations should be performed to give a precise location.

2.3 Tidal evolution

A close-in planet produces tidal bulges on the stellar surface, causing energy dissipation on the star and angular momentum exchanges between the stellar spin and planetary orbital motion. Meanwhile the star also generates tidal dissipation

on the planet, resulting in an eccentricity damping and orbital decay. For close-in planets with tidal dissipation factor $Q' \leq 10^6$, dissipation in planets dominates. The timescale of orbital circularization ($\tau_{\text{circ}} = e/\dot{e}$) induced by planetary tidal dissipation is given as (Mardling & Lin 2004, Zhou & Lin 2008),

$$\tau_{\text{circ}} = 2.4 \times 10^7 Q'_1 \left(\frac{a}{0.1\text{AU}}\right)^{\frac{13}{2}} \left(\frac{M_*}{M_\odot}\right)^{-\frac{3}{2}} \left(\frac{M}{M_\oplus}\right)^{-\frac{2}{3}} \left(\frac{\rho}{3\text{g cm}^{-3}}\right)^{\frac{5}{3}} \text{yr}, \quad (2.5)$$

where ρ is the density of the planet. The associate timescale of orbital decay ($\tau_{\text{decay}} = a/\dot{a}$) in elliptical orbits is

$$\tau_{\text{decay}} \approx \frac{1 - e^2}{2e^2} \tau_{\text{circ}}. \quad (2.6)$$

The orbital decay of a HSE under tidal dissipation determines its final location.

3 Examples systems

3.1 HD 40307 system

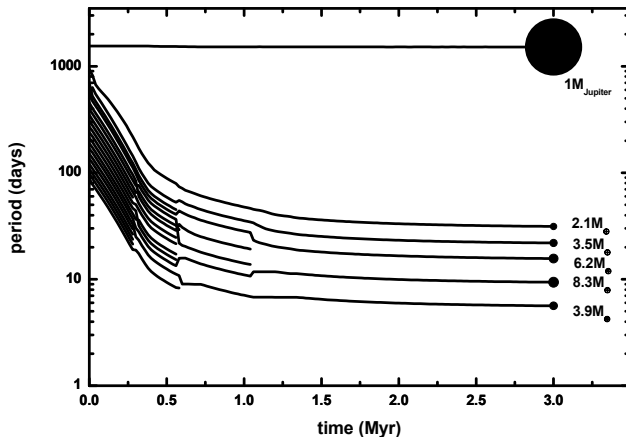


Fig. 2. Evolution of embryos in one run of simulation for HD 40307 system, where 20 embryos with initial isolation mass of Eq.(1.4) with $f_d = 6$ are put in inner orbits. A Jupiter mass planet is put at 2.4 AU without type II migration. Embryos undergo type I migration during evolution, with a reduction factor $C_1 = 0.3$ in Eq. (2.1).

The recent observed extra-solar planetary system around star HD40307 hosts three super-Earths with masses $4.2M_\oplus$, $6.9M_\oplus$, $9.2M_\oplus$ in orbits of 4.3days, 9.6 days and 20.5 days, respectively (Mayor et al. 2008). This configuration is very close to the Laplace resonance (with mean motion locking to 4 : 2 : 1) among the

three Galilean Satellites, Io-Europa-Ganymede, which is the only known example with such a configuration.

Lin et al. (2009) studied the formation of the HSEs in HD 40307 system. In situ formation of these planets requires a high density so that the disk must have been enhanced in refractory solids with $f_d > 25$, which is difficult to achieve in a gravitationally stable disk around a $0.8M_\odot$ and metal-deficient star. A compact system of embryos with smaller M_{iso} can formed under less extreme conditions and coagulate after the gas depletion. Fig.2 shows a typical run of N-body simulation with a Hermite-type code(Aarseth 2003). In this run a disk model of (1.1) and (1.2) with $f_g = 1$ and $f_d = 6$ are employed. In the inner region of disk, the column density increase near the boundary of MRI active-dead zone is considered(Kretke & Lin 2007). Reasonable parameters suitable for CTT stars estimate the boundary at around 20 days. We also assume that the disk has a exponential decay with a timescale of 1 Myr(Haicsh et al. 2001). We put initially 20 embryos with isolation masses from (1.4) and mutual separation of 7 Hill's radii, and one Jupiter mass giant planet located at 2.4 AU. After the evolution of 3 Myrs, the final system compose 5 super-Earths, with much smaller mutual separation. This simulation indicates that in situ formation of the three planets in HD 40307 system is unlikely.

Thus the most plausible scenario for their formation is (Lin et al. 2009): (i) formation of three planets in outside orbits; (ii) type I migration of the planets and the halt of migration of m_1 due to the density profile enhancement near the boundary of MRI active-dead zone(a_{mag}); the ongoing migration of m_2 and m_3 leads a consecutive trapping of 2:1 resonance with m_1 and m_2 , respectively, which results in a 4 : 2 : 1 configuration among the three planets, (iii) tidal evolution of three super-Earths during and after gas disk depletion to the present locations. As a typical run, Fig.3a shows that after the migration of m_1 is slowed down and stalled at a_{mag} at $T = 0.2$ Myr, the approaching m_2 enters into a 2:1 MMR at $T = 0.3$ Myr. Subsequently planet 3 is captured into m_2 's 2:1 MMR at $T = 0.6$ Myr, which results in a 4 : 2 : 1 resonance. However, if we increase the speed of type I migration by setting $C_1 = 0.3$ in Eq. (2.1), then the three planets will fall in a 6 : 3 : 2 resonance. A standard speed of type I migration ($C_1 = 1$) will reach a final configuration of 9 : 6 : 4. These results indicate clearly that the trap of mean motion resonance depends on the timescale of migration.

Fig.3b shows the subsequent tidal evolution of three planets initially from 4 : 2 : 1 resonance. Due to the tidal evolution and resonance interactions, the planets move inward while keeping the resonance configuration unchanged. This requires $\Delta a/a$ being the same for three planets, which is most difficult to follow for the outmost planet since its tidal dissipation is lowest. The configuration is broken at time $T \sim 0.7$ Myr when m_3 first leaves the resonance. The final configurations have periods of 4.35days, 9.53days, 20.15days, eccentricities of 0.016, 0.020,0.027 for m_1, m_2, m_3 , respectively. The relative errors of final periods compared with observational data of HD 40307 system are 0.9%, 0.9%1.5%, relatively. Due to the linear dependence of tidal force on Q' , the final state of circular orbits is achieved at time $T \sim 5Q'$ Myr. To compare with the observed circular orbits, this gives

a restriction of $Q' < 2000$ supposing an age of 10 Gyr for the star HD40307, indicating these HSEs are most likely rocky planets.

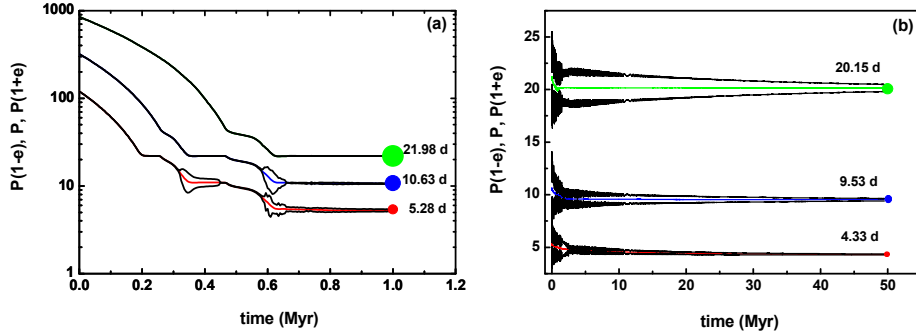


Fig. 3. Evolution of three super-Earths system around HD 40307 with reduced Type I migration speed, $C_1 = 0.1$ in Eq. 2.1. Three planets initially locate in circular orbits with periods of 120, 320, 850days. Panel (a) presents the evolution of $P(1+e)$, P , $P(1-e)$ of each planet, where P is the orbit period and e is the eccentricity. Panel (b) shows the tidal evolution of three super-Earths systems with an illustrative $Q' = 10$. Initially three planets are set in 4 : 2 : 1 MMR (with periods of 5.3days, 10.6days, 21.2days, respectively), with initial eccentricities 0.20 for all the three planets. From Lin et al. (2009).

3.2 GJ 436 system

GJ 436b is a Neptune-size planet with 23.2 Earth masses in an elliptical orbit of period 2.64 days and eccentricity 0.16 (Butler et al. 2004, Maness et al. 2007, etc). With a typical tidal dissipation factor ($Q' \sim 10^6$) as that of a giant planet with convective envelope, its orbital circularization timescale under internal tidal dissipation is around 1 Gyr, at least two times less than the stellar age (> 3 Gyr). Considering that radial velocities of GJ 436 reveal a long-term trend, Maness et al.(2007) proposed the presence of a long-period (~ 25 yr) planet companion with mass $\sim 0.27M_J$ (Jupiter mass) in an eccentric orbit ($e \sim 0.2$). Recently, Ribas et al.(2008) suggested that the observed radial velocities of the system are consistent with an additional small, super-Earth planet in the outer 2:1 mean-motion resonance with GJ 436b. More recent inspection of transit data implies that GJ 436b is perturbed by another planet with mass $\leq 12M_{\oplus}$ in a non-resonant orbit of ~ 12 days (Coughlin et al. 2008).

In Tong & Zhou (2009), we investigated extensively the possibility of the eccentricity excitation of GJ 436b by a companion, assuming the companion is either in a nearby/distant orbit, or in MMR with GJ 436b. Fig.4 shows the maximum eccentricity in parameter space that can be excited by the companion in nearby orbits. We find that, although the eccentricity of GJ 436b can be excited to 0.16

with a broad range of companion mass (above few Earth-masses), the maintain of the eccentricity to 0.16 under tidal dissipation is impossible. In fact, as the orbital decay time is short ($\sim 20\text{Gyr}$) for GJ 436b at the present location, significant orbital decay ($\sim 25\%$) is expect so that GJ 436b would be in a much closer orbit, and the eccentricity of GJ 436b would be damped within the stellar age. Distance companions can *not* excite and maintain the significant eccentricity of GJ 436b unless they are in highly eccentric orbits.

Based on the extensive investigations, we think the high eccentricity of GJ 436b can not be maintained by a companion in either nearby or distance orbits through secular perturbation or mean motion resonances. These results do *not* rule out the possible existence of planet companions in nearby/distance orbits, although they are not able to maintain the eccentricity of GJ 436b. Thus the maintaining of its eccentricity remains a challenge problem, unless GJ 436b has a extremely high dissipation factor ($Q' > 6 \times 10^6$).

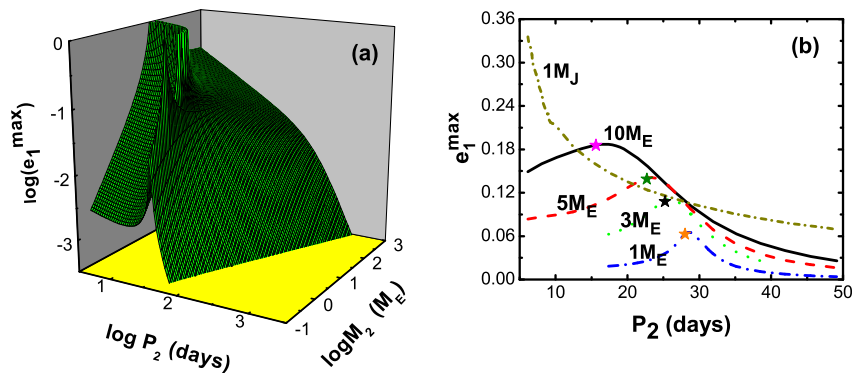


Fig. 4. Maximum eccentricity of GJ 436b that can be excited at the present location by a planet companion in outside orbit with initial eccentricity $e_2 = 0.2$. Panel (a): 3-D plot of $e_{1\max}$ in the plane of $P_2 - M_2$ from theoretical Eq. (2.4). Panel (b): $e_{1\max}$ obtained from numerical simulations of a general three-body model. The asterisks denote the singularities from Eq. (2.4). From Tong & Zhou (2009).

4 Conclusions

As more and more hot super-Earths (HSEs) are detected recently, with few multiple HSE systems, their formation story is not fully understood yet. For example, there exist several mysteries.

Retention of planetesimals and embryos under gas drag and disk tidal decay remains the major challenge. Although mechanisms have been proposed to stop the inward migration of Earth mass planet near the inner cavity of disk or near the boundary of MRI active-dead zone, the ubiquity of super-Earth plan-

ets at many other locations of the system merits explanation. If indeed they can only be stopped in the boundary MRI active-dead zone, or the inner cavity of disk, observation of HSEs can help to estimate such locations in the CTTS stage of protostars. During the later stage of planet formation, UVO photoevaporation from the host star or cosmic rays may severely deplete the gas disk, which will reduce the surface density of the disk by an order of magnitude at ~ 1 Myr (Alexander et al. 2006). Thus the migration speed is an order of magnitude lower than that estimate from the linear theory, embryos formed in the later stage could survive at more distant orbits.

Final configuration of Earth-mass planets. Most simulations of HSE formation indicates the presence of several super-Earths formed within mutual mean motion resonance (MMR) under type I migration. However, only HD 40307 system is observed to be near MMR. Tidal evolution will play part of the roles by removing such configurations, leaving the multiple planets in near resonance instead of the exact resonances. On the other hand, system with Earth mass planets far from resonance configurations are also present, like our solar system. Why type I migration seems to be not effective in such systems requires further investigations.

Acknowledgements I would like thank the organizers of the conference for their kind invitation. This work is supported by NSFC (10833001,10778603), National Basic Research Program of China (2007CB814800).

References

- Aarseth, S. J. 2003, *Gravitational N-Body Simulations*, (Cambridge: Cambridge University Press)
- Alexander, R. D., Clarke, C. J., Pringle, J. E., 2006, MNRAS, 369, 229
- Alibert Y. , Mordasini C., Benz W. , Winisdoerffer C., 2005, A&A 434, 343
- Balbus, S. A. , Hawley, J. F., 1991, ApJ, 376, 214-222
- Butler, R. P., Vogt, S. S., Marcy, G. W., et al., 2004, ApJ, 617, 580
- Coughlin, J. L., Stringfellow, G. S., Becker, A. C., et al., 2008, arXiv:0809.1664
- Fogg, M. J., Nelson, R. P., 2005, A&A, 441, 791
- Fogg M.J., Nelson R.P, 2007, A&A 472,1003
- Gammie C.F., 1996, ApJ 457,355
- Goldreich, P., Tremaine,S., 1979, ApJ, 233,857
- Haicsh,K.E.,Jr., Lada,E.A., Lada,C.J., 2001, ApJ,241, 425
- Hayashi,C. 1981, Prog. Theor.Phys. Suppl., 70,35
- Ida, S., Lin, D. N. C., 2004, ApJ, 604, 388
- Ida, S., Lin, D. N. C., 2008, ApJ, 673, 487
- Kokubo, E., Ida, S. 1996, Icarus, 123, 180
- Kokubo, E., Ida, S. 2002, ApJ, 581,666
- Königl,A., 1991, ApJ, 370,L39
- Kretke,K. A., Lin,D.N.C., 2007, ApJ, 664, L55
- Kretke, K. A., Lin, D. N. C., Garaud,P., Turner,N. J., 2009, ApJ, 690, 407.
- Lin, D.N.C., Zhou, J.L., Wang, S., Kretke, K. A., in preparation.

- Maness, H. L., Marcy, G. W., Ford, E. B., et al., 2007, *PASP*, 119, 90
- Mardling, R. A., 2007, *MNRAS*, 382, 1768
- Mardling, R., Lin, D. N.C. 2004, *ApJ*,614,955-959
- Masset, F.S. 2002 *A&A*,387,605
- Masset, F. S., Morbidelli, A., Crida, A., Ferreira, J. 2006,*ApJ*,642, 478
- Mayor,M., Udry,S., Lovis ,C. et al., 2009, *A & A*, 493, 639
- Morbidelli A., Crida, A., Masset, F., Nelson, R. P., 2008, *A&A* 478, 929
- Nagasawa, M., Lin, D. N. C., Thommes, E. 2005, *ApJ*, 635,578
- Pollack, J. B., Hubickyj, O., Bodenheimer, P., Lissauer, J. J., Podolack, M. & Greenzweig, Y. 1996, *Icarus*, 124, 62-85,
- Raymond, S. N., Barnes, R., Mandell, A. M., 2008, *MNRAS*, 384, 663
- Ribas, I., Font-Ribera, A., Beaulieu, J.-P., 2008, *ApJL*, 677, L59
- Safronov, V.S. 1969, *Evolution of the Protoplanetary Cloud and Formation of the Earth and the planets*, English translation NSSA TT F-677(1972)
- Shakura, N. I. , Sunyaev, R.A., 1973, *A&A* 24, 337
- Tanaka, H.,Takeuchi,T., Ward,W.R., 2002, *ApJ*, 565, 1257
- Terquem,C., Papaloizhou,J.B.C., 2007, *ApJ*,654,1110
- Tong,X. & Zhou,J.L., 2009, accepted by *Science in China (G): Physics, Mechanics and Astronomy*. arXiv 0812.3195.
- Ward, W.R., 1991, *Lunar Planet Sci. Conf.* 22, 1463
- Ward, W.R., 1993, *Icarus*, 106, 274
- Ward, W.R., 1997, *Icarus*, 126, 261
- Zhou, J.L., Aarseth, S. J., Lin, D. N. C., Nagasawa, M., *ApJ*, 631, L85
- Zhou, J.L., Lin, D.N.C., Sun,Y.S, 2007, *ApJ*, 666, 423
- Zhou, J.L. , Lin, D.N.C. 2008 in *Exoplanets: Detection, Formation and Dynamics*, eds: Sun,Y.S., Ferraz-Mello,S., Zhou,J. L., *Proc. of IAU Symp.* 249, Cambridge, Cambridge university Press, 2008, 285